Catalysis Today 138 (2008) 130–134

Contents lists available at ScienceDirect

Catalysis Today

journal homepage: www.elsevier.com/locate/cattod

Preparation of $Ni/Al_2O_3–ZrO_2$ catalysts and their application to hydrogen production by steam reforming of LNG: Effect of ZrO_2 content grafted on Al_2O_3

Jeong Gil Seo, Min Hye Youn, Ji Chul Jung, Kyung Min Cho, Sunyoung Park, In Kyu Song *

School of Chemical and Biological Engineering, Research Center for Energy Conversion and Storage, Seoul National University, Shinlim-dong, Kwanak-ku, Seoul 151-744, Republic of Korea

ARTICLE INFO

Article history:
Available online 3 July 2008

Keywords:
Alumina–zirconia
Nickel
Liquefied natural gas
Steam reforming
Hydrogen

ABSTRACT

$Al_2O_3–ZrO_2$ supports with various zirconium contents were prepared by grafting a trichelated zirconium precursor ($Zr(OBu)(CH_3COCHCOCH_3)_3$) on the surface of γ-$Al_2O_3$. $Ni/Al_2O_3–ZrO_2$ catalysts were then prepared by an impregnation method, and were applied to hydrogen production by steam reforming of liquefied natural gas (LNG). The effect of ZrO_2 content grafted on γ-Al_2O_3 on the catalytic performance of $Ni/Al_2O_3–ZrO_2$ catalysts was investigated. $Al_2O_3–ZrO_2$ prepared by a grafting method served as an efficient support for the nickel catalyst in the steam reforming of LNG. Both LNG conversion and H_2 composition in dry gas over $Ni/Al_2O_3–ZrO_2$ catalysts showed maximum values at a certain level of zirconium content. Among the catalysts tested, $Ni/Al_2O_3–ZrO_2$ (Zr/Al = 0.04) catalyst showed the best catalytic performance.

1. Introduction

Liquefied natural gas (LNG), which is abundant and mainly composed of methane, can serve as an alternate source for hydrogen production by steam reforming reaction. Although nickel-based catalysts have been widely used in the steam reforming reaction [1–6], they suffer from severe catalyst deactivation due to the sintering of nickel particles and the carbon deposition [3–6]. Several attempts for introducing various promoters have been made to improve the thermal and chemical stability of nickel-based catalysts [6–9]. Modification of support has also been attempted as one of the promising methods for improving the catalytic performance of nickel-based catalysts [10,11].

$Al_2O_3–ZrO_2$ supports prepared by grafting zirconium butoxide on the surface of Al_2O_3 were previously developed by this research group, and were employed as a support for a nickel catalyst in hydrogen production by steam reforming of LNG [10]. It is known that ZrO_2 acts as an oxygen supplier and steam adsorbent enhancing the catalytic performance of Ni-based catalysts in the reforming reactions [12,13]. For the practical application, however, the amount of ZrO_2 grafted on the surface of Al_2O_3 should be reduced due to the high cost of ZrO_2. It is expected that ZrO_2 can be finely dispersed on the surface of Al_2O_3 by controlling the hydrolysis rate of zirconium precursor. In this work, therefore, a trichelated zirconium precursor ($Zr(OBu)(CH_3COCHCOCH_3)_3$) instead of common zirconium alkoxide was used as a zirconium precursor for the preparation of $Al_2O_3–ZrO_2$ supports by a grafting method, with an aim of obtaining highly dispersed ZrO_2 on the surface of Al_2O_3. A series of $Al_2O_3–ZrO_2$ supports with various zirconium contents were prepared by a grafting method in this work. $Ni/Al_2O_3–ZrO_2$ catalysts were then prepared by an impregnation method for use in hydrogen production by steam reforming of LNG. The effect of ZrO_2 content grafted on Al_2O_3 on the performance of $Ni/Al_2O_3–ZrO_2$ catalysts in the steam reforming of LNG was investigated.

2. Experimental

$Al_2O_3–ZrO_2$ supports with various zirconium contents were prepared by grafting a zirconium precursor on the surface of γ-Al_2O_3 (Degussa), according to the similar method reported in the literature [10,14]. In this work, however, trichelated zirconium butoxide ($Zr(OBu)(CH_3COCHCOCH_3)_3$) obtained by the following reaction was used as a zirconium precursor. 2.4 ml of zirconium *sec*-butoxide (Aldrich) was added to 1.5 ml of 2,4-pentanedione

* Corresponding author. Tel.: +82 2 880 9227; fax: +82 2 889 7415.
E-mail address: inksong@snu.ac.kr (I.K. Song).

0920-5861/$ – see front matter © 2008 Elsevier B.V. All rights reserved.
doi:10.1016/j.cattod.2008.05.006

Table 1
Textural and chemical properties of Al_2O_3–ZrO_2 (AZX) supports

	AZ0	AZ1	AZ2	AZ3	AZ4
Zr used (wt.%)	0	15.2	30.4	45.6	60.8
Zr content (wt.%)[a]	0	3.1	4.1	5.9	6.7
Zr/Al atomic ratio[a]	0	0.03	0.04	0.05	0.06
Surface area (m^2/g)[b]	95	91	94	98	97
Pore volume (cm^3/g)[c]	0.25	0.21	0.33	0.17	0.13

[a] Measured by ICP-AES.
[b] BET surface area.
[c] BJH desorption pore volume.

(Aldrich) to obtain a clear solution of trichelated zirconium butoxide ($Zr(OBu)(CH_3COCHCOCH_3)_3$) in butanol.

$$Zr(OBu)_4 + 3CH_3COCH_2COCH_3 \rightarrow Zr(OBu)(CH_3COCHCOCH_3)_3 + 3BuOH \quad (1)$$

3 g of γ-Al_2O_3 (Degussa) was uniformly dispersed in 100 ml of anhydrous toluene (Aldrich). 0.6 ml of triethylamine (TEA, Fluka) was then added to the alumina slurry to activate the hydroxyl groups on the surface of alumina. The trichelated zirconium butoxide in butanol was slowly added to the alumina slurry with constant stirring, and the resulting slurry was stirred at room temperature for 6 h to achieve complete reaction of alumina with zirconium precursor. After removing the unreacted zirconium precursor by centrifugation, the slurry was washed several times with anhydrous toluene. Upon addition of an excess amount of deionized water to the washed slurry, a white gel was formed immediately. After maintaining the white gel in deionized water for 6 h, the solid was isolated by filtration. The solid product was dried overnight at 120 °C, and then it was calcined at 700 °C for 5 h to yield the Al_2O_3–ZrO_2 support. The prepared Al_2O_3–ZrO_2 supports were denoted as AZX (X = 1–4), where X is the number of times the overall grafting process was repeated. Ni/Al_2O_3–ZrO_2 catalysts were then prepared by impregnating a nickel precursor ($Ni(NO_3)_2{\cdot}6H_2O$, Aldrich) on AZ0 (γ-Al_2O_3) and AZX (X = 1–4) supports. The prepared catalysts were denoted as Ni/AZX (X = 0–4). The actual Ni loadings were 19.9 wt.% for Ni/AZ0, 20.3 wt.% for Ni/AZ1, 19.5 wt.% for Ni/AZ2, 21.2 wt.% for Ni/AZ3, and 20.0 wt.% for Ni/AZ4.

Chemical compositions of Al_2O_3–ZrO_2 (AZX) supports and nickel loadings in the Ni/Al_2O_3–ZrO_2 (Ni/AZX) catalysts were determined by ICP-AES (ICPS-1000IV, Shimadzu) analyses. Crystalline phases of supported catalysts and particle sizes of nickel species in the catalysts were examined by XRD (D-Max2500-PC, Rigaku) measurements using Cu-Kα radiation (λ = 1.541 Å) operated at 50 kV and 100 mA. In order to investigate the reducibility of supported nickel catalysts, temperature-programmed reduction (TPR) measurements by hydrogen were carried out in a conventional flow system equipped with a thermal conductivity detector (TCD) at temperatures ranging from room temperature to 1000 °C with a heating rate of 5 °C/min. Carbon deposition on the used catalysts was examined by TEM (JEM-2000EXII, Jeol) and CHNS elemental analyses (CHNS 932, Leco).

Steam reforming of LNG was carried out in a continuous flow fixed-bed reactor at 600 °C under atmospheric pressure. Prior to the catalytic reaction, each catalyst (100 mg) was reduced with a mixed stream of H_2 (3 ml/min) and N_2 (30 ml/min) at 700 °C for 3 h. Feed composition was fixed at CH_4:C_2H_6:H_2O:N_2 = 4.6:0.4:10:30, and total feed rate with respect to catalyst weight was maintained at 27,000 ml/h g. The reaction products were periodically sampled and analyzed using an on-line gas chromatograph (ACME 6000, Younglin) equipped with a TCD. LNG conversion and H_2 composition in dry gas were calculated according to the following equations on the basis of carbon balance.

$$\text{LNG conversion}\,(\%) = \left(1 - \frac{F_{CH_4,out} + F_{C_2H_6,out}}{F_{CH_4,in} + F_{C_2H_6,in}}\right) \times 100 \quad (2)$$

$$H_2\ \text{composition in dry gas}\,(\%) = \frac{F_{H_2,out}}{F_{H_2,out} + F_{CH_4,out} + F_{C_2H_6,out} + F_{CO,out} + F_{CO_2,out}} \times 100 \quad (3)$$

3. Results and discussion

Table 1 shows the textural and chemical properties of Al_2O_3–ZrO_2 (AZX) supports. The amount of ZrO_2 grafted on γ-Al_2O_3 was significantly less than that of zirconium source used. This is because γ-Al_2O_3 (AZ0) and as-synthesized Al_2O_3–ZrO_2 (AZX) supports have a limited number of hydroxyl groups to react with zirconium precursor [15]. Moreover, the three chelated ligands ($CH_3COCHCOCH_3$) suppressed the formation of three-dimensional and bulky ZrO_2 on the surface of γ-Al_2O_3 during the grafting process, resulting in relatively low zirconium content in the AZX (X = 1–4) supports. This is because the chelated ligands are not easily hydrolyzed compared to the butoxide ligand in the hydrolysis step [16]. It was found that surface areas of AZX supports were not significantly influenced by the addition of ZrO_2. This is due to the relatively low zirconium content in the AZX supports. Although pore volumes of AZX supports were in the range of 0.13 cm^3/g (AZ4)-0.33 cm^3/g (AZ2), these values showed no consistent trend with respect to the amount of ZrO_2 grafted.

Fig. 1 shows the XRD patterns of AZX (X = 0–4) supports calcined at 700 °C. The prepared AZX (X = 1–4) supports showed the characteristic diffraction peaks of γ-Al_2O_3 phase, which were almost identical to those of AZ0 support. It is interesting to note that AZX (X = 1–3) supports showed no diffraction peaks corresponding to ZrO_2, indicating high dispersion of ZrO_2 on the surface of γ-Al_2O_3. However, AZ4 showed weak diffraction peaks indicative of tetragonal phase of ZrO_2. This is believed to be due to the fact that AZ4 retained relatively high zirconium content (Zr/Al = 0.06).

Fig. 2 shows the XRD patterns of Ni/AZX (X = 0–4) catalysts calcined at 700 °C. Ni/AZX (X = 0–4) catalysts showed the characteristic diffraction peaks of NiO species (dashed lines). A close examination of the diffraction peaks revealed that the (440) diffraction peak of γ-Al_2O_3 (solid line) shifted to a lower diffraction

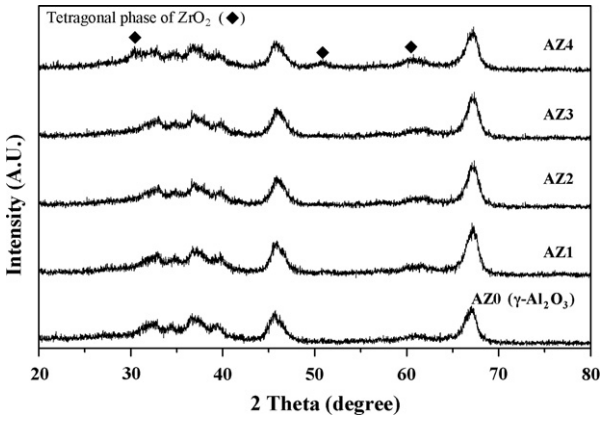

Fig. 1. XRD patterns of AZX (X = 0–4) supports calcined at 700 °C.

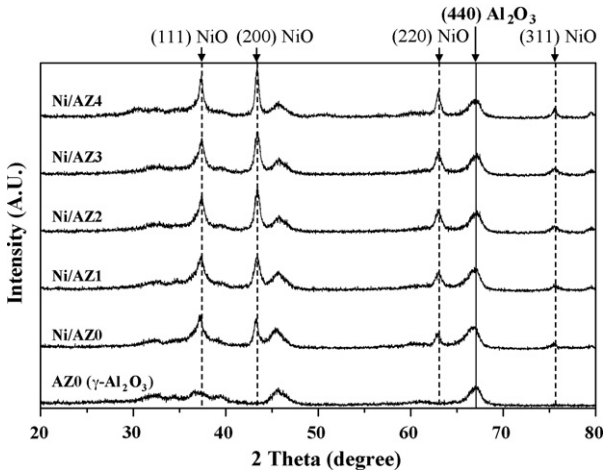

Fig. 2. XRD patterns of Ni/AZX (X = 0–4) catalysts calcined at 700 °C.

angle in the Ni/AZ0. This is due to the lattice expansion of γ-Al_2O_3 caused by the incorporation of Ni^{2+} into the lattice of γ-Al_2O_3 [17,18]. However, the shift of (440) diffraction peak of γ-Al_2O_3 in the Ni/AZX (X = 1–4) catalysts became smaller or negligible with increasing ZrO_2 content. Lattice parameters of AZ0 (γ-Al_2O_3) support and Ni/AZX (X = 0–4) catalysts calculated from XRD peaks are listed in Table 2. The lattice parameter of Ni/AZ0 (=0.793) was greater than that of AZ0 (γ-Al_2O_3) (=0.790). On the other hand, the Ni/AZ1 exhibited a slightly smaller lattice parameter than the Ni/AZ0. Furthermore, the lattice parameter of Ni/AZX (X = 2–4) catalysts was identical to that of AZ0 (=0.790). This result indicates that the incorporation of Ni^{2+} into the lattice of γ-Al_2O_3 in the Ni/AZX (X = 1–4) catalysts was suppressed by the new interaction between ZrO_2 and γ-Al_2O_3. Particle size and dispersion of nickel species in the Ni/AZX (X = 0–4) catalysts are listed in Table 3 [19]. It was found that the Ni/AZ0 exhibited large particle size (32.1 nm) and poor dispersion (3.0%). On the other hand, the Ni/AZX (X = 1–3) catalysts retained smaller particle size and higher dispersion than the Ni/AZ0 catalyst. Although the addition of zirconia weakened the interaction between nickel species and alumina support, small amount of zirconia acted as a spacer or barrier which prevented the aggregation of nickel species for fine dispersion [20]. However, relatively large amount of zirconia in the Ni/AZ4 catalyst was not favorable for fine dispersion of nickel species.

Fig. 3 shows the TPR profiles of Ni/AZX (X = 0–4) catalysts. Ni/AZ0 catalyst showed a broad reduction peak at around 820 °C, corresponding to the reduction of nickel aluminate-like phase. The reduction peak temperature of Ni/AZX (X = 0–2) catalysts shifted to a lower temperature with increasing zirconium content. In other words, the interaction between nickel species and support was weakened by the new interaction between highly dispersed ZrO_2 and γ-Al_2O_3 in the Ni/AZ1 and Ni/AZ2 catalysts. On the other hand, both Ni/AZ3 and Ni/AZ4 catalysts exhibited a higher reduction peak temperature than Ni/AZ2 catalyst, but they still showed a lower reduction peak temperature than Ni/AZ0 catalyst. Among the catalysts examined, Ni/AZ2 catalyst showed the highest reducibility (the lowest reduction peak temperature).

Table 2
Lattice parameters of AZ0 (γ-Al_2O_3) support and Ni/AZX (X = 0–4) catalysts

Sample	Lattice parameter (nm)
AZ0 (γ-Al_2O_3)	0.790
Ni/AZ0	0.793
Ni/AZ1	0.792
Ni/AZ2	0.790
Ni/AZ3	0.790
Ni/AZ4	0.790

Table 3
Particle size and dispersion of nickel species in the Ni/AZX (X = 0–4) catalysts

Catalyst	Particle size of nickel species (nm)[a]	Dispersion of nickel species (%)[b]
Ni/AZ0	32.1	3.0
Ni/AZ1	20.2	4.8
Ni/AZ2	19.9	4.9
Ni/AZ3	19.8	4.9
Ni/AZ4	34.5	2.8

[a] Calculated by Scherrer equation using (311) diffraction peak of nickel oxide.
[b] Dispersion (%) = 971/particle diameter (Å) [19].

Fig. 4 shows the LNG conversion with time on stream over selected Ni/AZX (X = 0, 2, and 4) catalysts in the steam reforming of LNG at 600 °C. It was difficult to find an accurate theoretical equilibrium LNG conversion using commercial simulators due to their different database [21,22]. Ni/AZ0 catalyst experienced a severe catalyst deactivation during the reaction. However, both Ni/AZ2 and Ni/AZ4 catalysts showed a stable catalytic performance during the reaction extending over 1000 min. Although the catalytic performances of Ni/AZ1 and Ni/AZ3 were not shown in Fig. 4, they also exhibited a stable catalytic performance during the reaction. CHNS elemental analyses were performed to quantify the amount of carbon deposition on the Ni/AZX (X = 0–4) catalysts. The amount of carbon deposited on the Ni/AZ0 catalyst after a 1000-min reaction was 12 wt.%, while that deposited on the Ni/AZX (X = 1–4) catalysts was less than 0.3 wt.%. The carbon deposition on

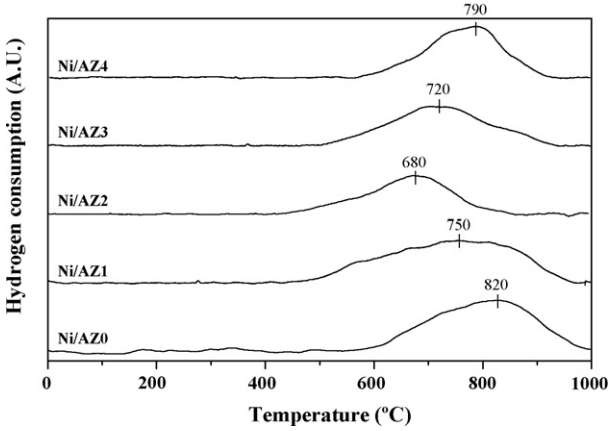

Fig. 3. TPR profiles of Ni/AZX (X = 0–4) catalysts.

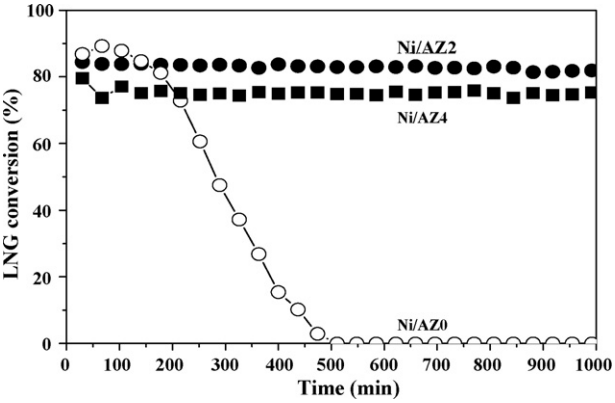

Fig. 4. LNG conversion with time on stream in the steam reforming of LNG over selected Ni/AZX (X = 0, 2, and 4) catalysts at 600 °C.

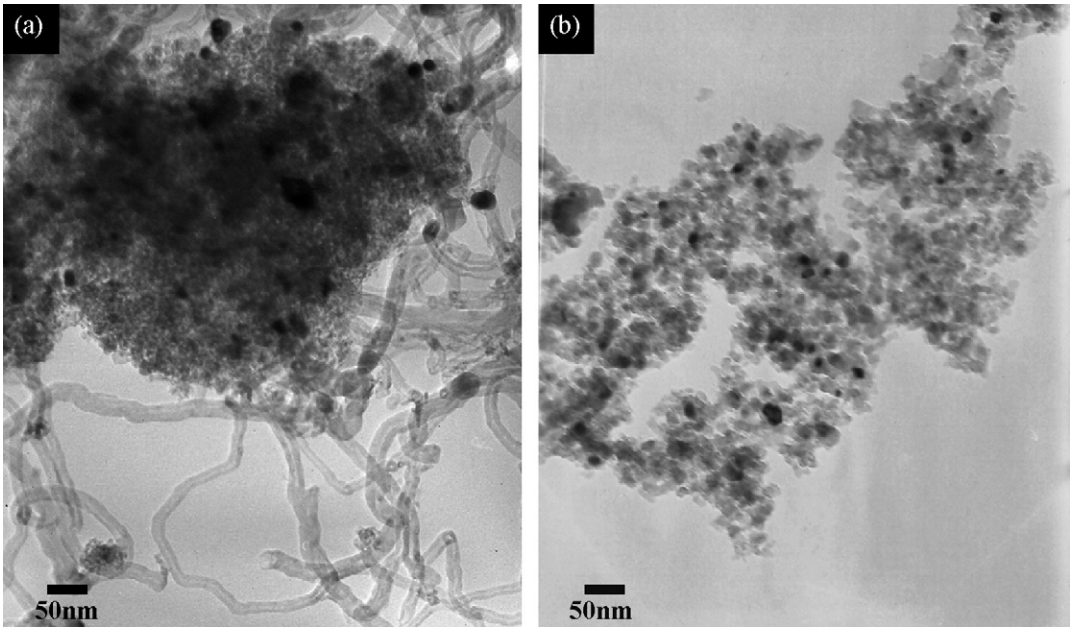

Fig. 5. TEM images of (a) Ni/AZ0 and (b) Ni/AZ2 catalysts after a 1000-min reaction.

the catalyst surface was further confirmed by TEM images, as shown in Fig. 5. Ni/AZ0 catalyst showed the filamentous carbon derived from a significant amount of carbon deposited during the steam reforming of LNG. On the other hand, Ni/AZ2 catalyst showed no considerable carbon deposition.

The reasons why Ni/AZX (X = 1–4) catalysts show a better catalytic performance than Ni/AZ0 catalyst can be explained by the effect of ZrO_2. It is known that the oxygen mobility of ZrO_2 is higher than that of γ-Al_2O_3, and therefore, ZrO_2 acts as an efficient oxygen supplier [23]. It is believed that ZrO_2 played an important role in facilitating the spillover of adsorbed steam from the support to the active nickel. The migrated steam, in turn, enhanced the gasification of surface hydrocarbons or carbon species, resulting in an improved catalytic performance of Ni/AZX (X = 1–4) catalysts. Furthermore, highly dispersed ZrO_2 in the Ni/AZX (X = 1–4) catalysts prevented the formation of inactive nickel aluminate-like phase through the formation of favorable Al_2O_3–ZrO_2 composite structure, as evidenced by XRD (Figs. 1 and 2) and TPR (Fig. 3) measurements.

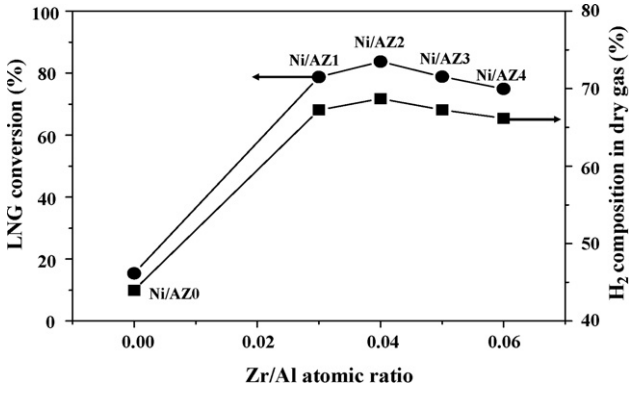

Fig. 6. LNG conversion and H_2 composition in dry gas as a function of Zr/Al atomic ratio over Ni/AZX (X = 0–4) catalysts in the steam reforming of LNG at 600 °C. Data were obtained after a 400-min reaction.

Fig. 6 shows the LNG conversion and H_2 composition in dry gas as a function of Zr/Al atomic ratio over Ni/AZX (X = 0–4) catalysts in the steam reforming of LNG at 600 °C. Both LNG conversion and H_2 composition in dry gas over Ni/Al_2O_3–ZrO_2 catalysts showed maximum values at a certain level zirconium content. Among the catalysts tested, Ni/AZ2 (Zr/Al = 0.04) catalyst showed the best catalytic performance. Although the reducibility of the catalyst is not the sole factor determining the catalytic performance in the steam reforming of LNG, both LNG conversion and H_2 composition in dry gas increased with increasing reducibility of the catalyst (the correlations can be established from Figs. 3 and 6, although they are not shown here). Among the catalysts tested, Ni/AZ2 catalyst with the highest reducibility (with the lowest reduction peak temperature) showed the best catalytic performance. The above results imply that an optimum ratio of Zr/Al was required for the best catalytic performance of Ni/AZX (X = 0–4) catalysts in the steam reforming of LNG.

4. Conclusions

Al_2O_3–ZrO_2 (AZX) supports with highly dispersed ZrO_2 were successfully prepared by grafting a trichelated zirconium precursor ($Zr(OBu)(CH_3COCHCOCH_3)_3$) on the surface of γ-Al_2O_3. ZrO_2 inhibited the incorporation of Ni^{2+} into the lattice of γ-Al_2O_3 through the formation of favorable Al_2O_3–ZrO_2 composite structure. Al_2O_3–ZrO_2 composite support enhanced the adsorption of steam and the subsequent spillover of steam from the support to the active nickel during the reaction. In the steam reforming of LNG, both LNG conversion and H_2 composition in dry gas showed maximum values at a certain level of zirconium content. Among the catalysts tested, Ni/AZ2 catalyst showed the best catalytic performance. It is concluded that an optimum ratio of Zr/Al was required for the maximum catalytic performance of Ni/AZX catalysts in the steam reforming of LNG. The reducibility of Ni/AZX catalysts was also partly responsible for the catalytic performance in hydrogen production by steam reforming of LNG.

Acknowledgements

The authors wish to acknowledge support from the Seoul Renewable Energy Research Consortium (Seoul R & BD Program) and RCECS (Research Center for Energy Conversion and Storage: R11-2002-102-00000-0).

References

[1] J.K. Lee, D. Park, Korean J. Chem. Eng. 15 (1998) 658.
[2] K.D. Ko, J.K. Lee, D. Park, S.H. Shin, Korean J. Chem. Eng. 12 (1995) 478.
[3] J.R. Rostrup-Nielsen, Catal. Today 63 (2000) 159.
[4] O. Yokota, Y. Oku, T. Sano, N. Hasegawa, J. Matsunami, M. Tsuji, Y. Tamaura, Int. J. Hydrogen Energy 25 (2000) 81.
[5] K.O. Christensen, D. Chen, R. Lødeng, A. Holmen, Appl. Catal. A 314 (2006) 9.
[6] T. Borowiecki, A. Gołębiowski, B. Stasińska, Appl. Catal. A 153 (1997) 141.
[7] T. Borowiecki, W. Gac, A. Denis, Appl. Catal. A 270 (2004) 27.
[8] J.S. Lisboa, D.C.R.M. Santos, F.B. Passos, F.B. Noronha, Catal. Today 101 (2005) 15.
[9] M.E.S. Hegarty, A.M. O'Connor, J.R.H. Ross, Catal. Today 42 (1998) 225.
[10] J.G. Seo, M.H. Youn, I.K. Song, J. Mol. Catal. A 268 (2007) 9.
[11] F. Pompeo, N.N. Nichio, O.A. Ferretti, D. Resasco, Int. J. Hydrogen Energy 30 (2005) 1399.
[12] Y. Matsumura, T. Nakamori, Appl. Catal. A 258 (2004) 107.
[13] R. Takahashi, S. Sato, T. Sodesawa, M. Yoshida, S. Tomiyama, Appl. Catal. A 273 (2004) 211.
[14] J.G. Seo, M.H. Youn, I.K. Song, J. Power Sources 168 (2007) 251.
[15] P. Iengo, M.D. Serio, V. Solinas, D. Gazzoli, G. Salvio, E. Santacesaria, Appl. Catal. A 170 (1998) 225.
[16] M. Chatry, M. Henry, J. Livage, Mater. Res. Bull. 29 (1994) 517.
[17] T. Ueckert, R. Lamber, N.I. Jaeger, U. Schubert, Appl. Catal. A 155 (1997) 75.
[18] G. Li, L. Hu, J.M. Hill, Appl. Catal. A 301 (2006) 16.
[19] J. Bartolomew, J. Catal. 65 (1980) 73.
[20] S. Natesakhawat, R.B. Watson, X. Wang, U.S. Ozkan, J. Catal. 234 (2005) 496.
[21] S. Rakass, H. Oudghiri-Hassani, P. Rowntree, N. Abatzoglou, J. Power Sources. 158 (2006) 485.
[22] Y.-S. Seo, A. Shirley, S.T. Kolaczkowski, J. Power Sources. 108 (2002) 213.
[23] D. Duprez, Stud. Surf. Sci. Catal. 112 (1997) 13.